A Simple Apparatus for Studies of Thermoprogrammed Desorption in Solution

F. Salvador* and M. D. Merchán

Departamento de Química Física, Facultad de Química, Universidad de Salamanca, 37008 Salamanca, Spain

Received July 17, 1991. In Final Form: February 7, 1992

A description is given of the design and construction of an experimental thermoprogrammed desorption apparatus for the study of desorption in solution. The work offers some of the thermograms obtained for the desorption of crystal violet from silica gel and activated charcoal and also of certain phenol derivatives adsorbed on charcoal. All thermograms point to the possibility of the application of this technique to condensed phase desorption. The most noteworthy differences observed between thermodesorption in solution and in the gaseous phase are discussed.

Introduction

Since its appearance in the 1940s with flash desorption, temperature programmed desorption (TPD) has proved to be one of the most valid techniques in the investigation of the surfaces of adsorbents and catalysts. However, this is not its only application, since of equal or greater importance is the information that one can obtain through a detailed analysis of desorption kinetics.

From the very beginnings of TPD, numerous studies focused on the identification of the different states of adsorption and for the calculation of their activation energies. The first quantitative results refer to the desorption of N_2 from tungsten[1-4] and to that of H_2[3,5,6] and CO[4,7,8] from tungsten, too. The technique was later extended to the study of catalytic processes on metallic surfaces such as the desorption of ethylene, acetylene, and methane on platinum, iridium, and tungsten[9-11] and to heterogeneous catalysts. In the latter field, of interest are the many works of Amenomiya and Cvetanovic[12-14] who used alumina as the adsorbent. Other heterogeneous adsorbents studied are activated charcoal and silica gel,[15,16] as well as other metal oxides (MoO_3, NiO, ZnO, TiO_2, etc.).[17-26] More recently, this technique has been employed for the characterization of supported metals[20,27,28] and of zeolites; the works in this field are numerous.[29-35]

The theoretical aspects of the thermal desorption of gas are well documented, in the work of Redhead[36] and Ehrlich.[37] Currently, there are numerous proposals for new models and methods for the calculation of kinetic parameters.[38-44]

As may be inferred from the foregoing and from a previous study[45] describing the development of TPD, since its beginnings until the present, this technique has been systematically applied in studies in which the adsorbent or catalyst is in contact with the adsorbate in the gaseous phase. Until now, the extension of this to other cases, in which the adsorbate is in solution, has not been assayed; this might be due to the experimental difficulty involved in subjecting the samples to high temperatures to achieve desorption and, in turn, to maintaining the system in the condensed phase or to the generally less well developed research on adsorption in solution.

The aim of the present work was to construct and put into operation an experimental setup that would permit us to carry out thermal desorption in solution (TPD-S) and to offer some of the results to validate the application of the technique in the condensed phase. The most pronounced differences observed between TPD in the gaseous phase and in solution TPD-S are also discussed.

(1) Ehrlich, G. *J. Chem. Phys.* **1955**, *23*, 1543.
(2) Ehrlich, G. *J. Phys. Chem.* **1956**, *60*, 1388.
(3) Hickmott, T. W.; Ehrlich, G. *J. Phys. Chem. Solids* **1958**, *5*, 47.
(4) Rigby, L. J. *Can. J. Phys.* **1964**, *42*, 1256.
(5) Tamm, P. W.; Schmidt, L. D. *J. Chem. Phys.* **1969**, *51*, 5352.
(6) Tamm, P. W.; Schmidt, L. D. *J. Chem. Phys.* **1971**, *54*, 4775.
(7) Hickmott, T. W. *J. Chem. Phys.* **1960**, *32*, 810.
(8) Yates, J. T., Jr.; King, D. A. *Surf. Sci.* **1972**, *32*, 479.
(9) Hansen, R. S.; Arthur, J. R., Jr.; Mimeault, V. J.; Rye, R. R. *J. Phys. Chem.* **1966**, *70*, 2787.
(10) Rye, R. R.; Hansen, R. S. *J. Chem. Phys.* **1969**, *50*, 3585.
(11) Berlowitz, P.; Megiris, C.; Butt, J. B.; Kung, H. H. *Langmuir* **1985**, *1*, 206.
(12) Amenomiya, Y.; Cvetanovic, R. J. *J. Phys. Chem.* **1963**, *67*, 144.
(13) Amenomiya, Y.; Cvetanovic, R. J. *J. Phys. Chem.* **1963**, *67*, 2046.
(14) Amenomiya, Y.; Cvetanovic, R. J. *J. Phys. Chem.* **1963**, *67*, 2705.
(15) Rivin, D.; Illinger, J. L. *J. Colloid Interface Sci.* **1969**, *31*, 85.
(16) Illinger, J. L.; Rivin, D. *Surf. Sci.* **1970**, *21*, 169.
(17) Yakerson, V. I.; Rozanov, V. V.; Rubinshtein, A. M. *Surf. Sci.* **1968**, *12*, 221.
(18) Munuera, G. *J. Catal.* **1970**, *18*, 19.
(19) Baranski, A.; Cvetanovic, R. J. *J. Phys. Chem.* **1971**, *75*, 208.
(20) Menon, P. G.; De Paw, R. P.; Froment, G. F. *Ind. Eng. Chem. Prod. Res. Dev.* **1979**, *18*, 110.
(21) Belokopytov, Yu. V.; Grebennikov, Yu, N.; Korneichuk, G. P. *React. Kinet. Catal. Lett.* **1981**, *16*, 409.
(22) Cheng, W. H.; Kung, H. H. *Surf. Sci.* **1982**, *122*, 21.
(23) Belokopytov, Yu. V.; Grebennikov, Yu. N.; Pyatniskii, Yu. I.; Telyatnik, A. I. *React. Kinet. Catal. Lett.* **1983**, *23*, 99.
(24) Cheng, W. H.; Akhter, S.; Kung, H. H. *J. Catal.* **1983**, *82*, 341.
(25) Farneth, W. E.; Ohuchi, F.; Staley, R. H.; Chowdhry, U.; Sleight, A. W. *J. Phys. Chem.* **1985**, *89*, 2493.
(26) Farneth, W. E.; Staley, R. H.; Sleight, A. W. *J. Am. Chem. Soc.* **1986**, *108*, 2327.
(27) Anderson, J. R.; Foger, K.; Breakspere, R. J. *J. Catal.* **1979**, *57*, 458.
(28) Hernandez, J. O.; Choren, E. A. *Rev. Téc. Fac. Ing., Univ. Zulia* **1983**, *6*, 58.
(29) Hoffmann, J.; Hunger, B.; Barth, A. *Z. Chem.* **1979**, *19*, 389.
(30) Dombrowski, V. D.; Hoffmann, J.; Hunger, B.; Barth, A. *Z. Phys. Chem.* **1980**, *261*, 649.
(31) Topsoe, N.-Y.; Pedersen, K.; Derouane, E. G. *J. Catal.* **1981**, *70*, 41.
(32) Hunger, B.; Hoffmann, J. *J. Therm. Anal.* **1983**, *27*, 353.
(33) Scholle, K. F. M. G. J.; Kentgens, A. P. M.; Veeman, W. S.; Frenken, P.; Van Der Velden, G. P. M. *J. Phys. Chem.* **1984**, *88*, 5.
(34) Hunger, B.; Hoffmann, J. *Thermochim. Acta* **1985**, *92*, 189.
(35) Hunger, B.; Hoffmann, J. *Thermochim. Acta* **1986**, *106*, 133.
(36) Redhead, D. A. *Vacuum* **1962**, *12*, 203.
(37) Ehrlich, G. *Adv. Catal.* **1963**, *14*, 255.
(38) Joly, J. P. *C. R. Acad. Sci.* **1982**, *295*, 717.
(39) Munteanu, G.; Segal, E. *Thermochim. Acta* **1985**, *89*, 187.
(40) Hashimoto, K.; Masuda, T.; Mori, T. *Stud. Surf. Sci. Catal.* **1986**, *28*, 503.
(41) Miller, J. B.; Siddiqui, H. R.; Gates, S. M.; Russell, J. N., Jr.; Yates, J. T., Jr.; Tully, J. C.; Cardillo, M. J. *J. Chem. Phys.* **1987**, *87*, 6725.
(42) Tronconi, E.; Lietti, L. *Surf. Sci.* **1988**, *199*, 43.
(43) Leary, K. J.; Michaels, J. N.; Stracy, A. M. *AIChE J.* **1988**, *34*, 263.
(44) Ioannides, T.; Verykios, X. E. *J. Catal.* **1989**, *120*, 157.
(45) Merchán, M. D.; Salvador, F. *Studia Chem.* **1990**, *15*, 127.

0743-7463/92/2408-1226$03.00/0

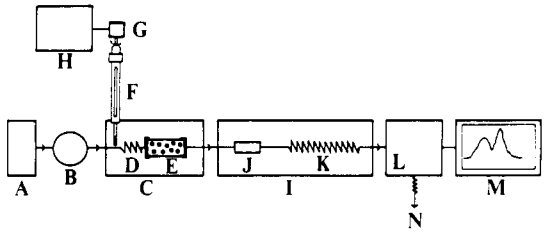

Figure 1. Scheme of apparatus: A, reservoir of carrier fluid; B, high-pressure pump; C, silicone oil bath; D, preheater; E, chamber of desorption; F, contact thermometer; G, reducing motor; H, temperature programmer; I, constant temperature bath; J, protective filter; K, refrigerant; L, UV–vis spectrophotometer; M, recorder; N, exit drainage.

Methods

Briefly, a TDP apparatus for gases functions as follows: The substrate is placed in a desorption chamber and is heated in an oven fitted with a temperature control. The particles are removed from the surface by the thermal excitation due to the temperature. The desorbed particles are removed from the chamber by a vacuum or by a carrier gas. The desorption process is detected by measuring the increase in pressure or, more specifically, by mass spectrometric determination of the flow of desorbed molecules.

In the case of TDP-S the apparatus constructed is shown in Figure 1. It functions in a similar way to that described for gases. However, the marked differences between the handling of liquids and gases mean that the characteristics of its components are completely different. The most singular part of the apparatus is that placed between the pump (B) and the cooling coil (K), which consists of a zone of high pressure since the main idea of the method is to maintain the system at high pressures during the heating phase so that the sample will remain in the condensed phase throughout the procedure. Such conditions were achieved in a very simple way, using a very long and narrow tube as the coil; with this, the loss of charge in the circulating fluid is quite considerable, thereby increasing the pressure in the desorption chamber (E). This, however, means that a high-pressure pump is required.

In the apparatus, the carrier fluid, stored in the reservoir (A), is impelled by a pump (B) of the kind used in HPLC; namely a Model KNK-50 supplied by KONIK with digital readings of flows and pressures. The flow rates offered by the system range between 10 μL and 5 cm^3/min. The maximum pressure tolerated by this pump is 500 atm. Periodic controls were carried out to check flow rate in order to guarantee a constant flow of carrier liquid.

The cylindrical desorption chamber (E), 4 cm in length and with a capacity of 1.0 cm^3, was constructed of stainless steel alloy 316 with a 3 mm thick wall. The desorption chamber is closed with two screw caps at either end that permit circulation of the carrier fluid through them. Both screw caps also contain filter plates (also of stainless steel; 2 μm and $^1/_4$ in. diameter) to ensure that the adsorbent will remain in the desorption chamber. This design was chosen in view of the ease in filling and emptying the chamber and its resistance to high temperatures and the high thermal conductivity of stainless steel. The chamber rests in a constant temperature bath (C) of silicone oil (Tamson, Model TC-3) of 3-L capacity, in this case specially designed to be able to work at high temperatures (up to 300 °C). A device was fitted for vigorous stirring such that it was possible to achieve a rapid equaling of temperature.

Thermoprogramming is achieved by twisting the upper knob of the contact thermometer (F) of the bath. A small reducing motor (G) turns this control slowly at a constant rate. With this it is possible to ensure that the rise of the mercury contact will be uniform and hence that the heating rate will be linear. The motor chosen is a type 117 manufactured by Cramer Division, Old Saybrook, CT; its rotation speed is 1 rpm such that a heating rate of 1.12 K/min is achieved. Owing to its characteristics it is possible to add an electronic device (H) able to modify the number of cycles of the electric current that the motor receives, thereby enabling one to vary the turning rate, and hence the heating rate,

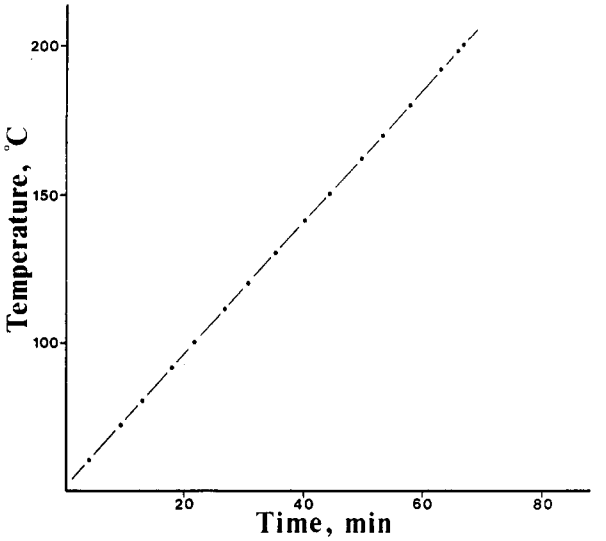

Figure 2. Least-squares fitting for a linear heating: slope = $2.2242 \pm 7.2 \times 10^{-4}$ °C/min; intercept = 51.01 ■ 0.03 °C, correlation coefficient = 0.999 997.

at will. The apparatus has been constructed before and has been applied in nonisothermic kinetic studies.[46-49] Suitably modified, it allowed us to cover a range of heating rates between 0.4 and 4.0 K/min.

To control temperature, a mercury thermometer (0–350 °C) with a sensitivity of ±0.25 °C was fitted. This is submerged in the thermostated bath. The different heating rates were determined by linear adjustment of temperature over time by the least-squares method. Figure 2 shows one of these correlations. From the goodness of fit one determines the correct functioning of the temperature programming.

To guarantee that the carrier fluid penetrating the desorption chamber will be at the temperature imposed by the programmer, a preheater (D) was placed immediately before the desorption chamber (E); this consists of a coil constructed of a stainless steel capillary tube 1 m in length with an inner diameter of 0.5 mm.

At the exit of the desorption chamber there is a high-pressure protective filter (J) (Hastelloy C (R) SII 0.5–0.125, with a 0.5-μm pore size and 6.4 cm^2 surface area). This filter is inserted to avoid obstruction of the circuit or damage to the detector by particles of the adsorbent. The filter is submerged in a cryostatic bath (I) (Heto) to protect it from the high temperatures reached by the carrier fluid. After this, in the same bath, there is a long refrigerating coil (K) whose mission is to cool the desorbed species to a constant temperature close to 25 °C before entering the detector (L) and to increase the loss of charge of the carrier liquid. The refrigerating system is built of a 6 m long stainless steel tube of 0.25 mm i.d. Using these conditions and flow rates of 4 cm^3/min, it is possible to achieve pressure above 100 atm in the desorption chamber. The minimum working pressure to maintain the condensed phase is a function of the temperature reached at each moment. This can be determined from the liquid–vapor balance curve of the carrier liquid used. Accordingly, there will be a limitation to the maximum working temperature that is imposed by the critical temperature of the carrier liquid. Thus, in the case of water this temperature is 647 K, which makes it necessary to work with a minimum pressure of 218 atm.

Detection of the desorbed sample is achieved with a UV–vis detector (Kratos 757) with which it is possible to work at different absorbance sensitivities (0.005–2). The wavelength precision was 0.5 nm. The detector has a SFA-235 flow cell of 5 mm optical pathway and a volume of 12 μL; an identical cell was used as

(46) Gonzalez, J. L.; Salvador, F. *React. Kinet. Catal. Lett.* **1982**, *21*, 167.
(47) Salvador, F.; Gonzalez, J. L. *React. Kinet. Catal. Lett.* **1984**, *25*, 125.
(48) Salvador, F.; Salvador, A. *React. Kinet. Catal. Lett.* **1984**, *26*, 311.
(49) Salvador, F.; Gonzalez, J. L.; Tel, L. M. *J. Chem. Educ.* **1985**, *62*, 613.

reference. All connections between the different parts of the circuit were made with conical joints designed to bear high pressures.

Plotting of the desorption rates, in units of absorbance, against temperature (thermogram) was made on a linear scale Servoscrive IS, Model RE 543.20 potentiometer (0–100%), with a response time of 0.5 s. The effect of temperature is 0.1% every 10 K. It has a time base with different chart speeds (3–300 cm/h).

At the exit of the detector a draining device (N) of 2 m length was installed. This, apart from allowing recovery of the sample desorbed, afforded the last part of the circuit a slight loss of charge, thus avoiding the appearance of bubbles in the detector cuvette.

It should be noted that in the studies performed with crystal violet, it was observed that the stainless steel circuit was not completely inert and retained some of the dye in the filters and in the cooling coil (K). Accordingly, in the current study titanium filters ($^1/_{16}$ in. o.d., 0.3 mm i.d.) were employed together with steel tubing covered inside with glass (supplied by ALLTECH). These modifications afforded a completely inert apparatus, although its construction and handling proved to be more delicate.

The activated and weighed adsorbent was placed in a reaction flask and subjected to gentle stirring in a concentrated aqueous solution of the adsorbate. Periodic monitoring of the solution allowed us to determine the degree of adsorption. The adsorbents assayed with this apparatus were granular activated charcoal (20–40 mesh) from Aldrich and silica gel for chromatography (35–70 mesh), from Merck. Prior to its saturation the activated charcoal was washed with boiling water and outgassed by heating at 150 °C over 48 h. The silica gel was also activated by heating at 150 °C. The adsorbates crystal violet, phenol, *p*-nitrophenol, and 2,6-dichloro-4-nitrophenol, were from Sigma. In view of the low concentrations used for the case of crystal violet and the purity of this compound, it was employed as received from the manufacturer. The phenol and phenol derivatives were purified by recrystallization in water. Bidistilled filtered water was used as the solvent and carrier fluid.

The method for obtaining the thermograms was always the same: A small amount of saturated adsorbate is introduced into the desorption chamber. Once filled and closed, the chamber is placed in the silicone bath, and the pump was immediately started. When steady state is reached with respect to temperature and the detector signal, the temperature programmer is connected. At this moment a chronometer is started to be able to record the variations in temperature over time. Temperature is read on a mercury thermometer submerged in the thermostatic bath.

In order to check the stability of the adsorbate against temperature, samples of desorbed adsorbate are collected periodically through the drainage system of the apparatus (N) and analyzed in a spectrophotometer (in our case a Shimadzu UV-240) where the complete UV–vis spectrum is recorded. At temperatures above those reached in the thermograms obtained, the four desorbed species show alterations and displacements of their spectral maxima toward lower wavelengths.

Results

Figure 3 shows the thermogram corresponding to the desorption of a dye, crystal violet, from silica gel. A single peak is observed together with a single activation energy of desorption with a very well-defined maximum at a relatively low temperature (367 K). This indicates a weak binding of the dye. Desorption occurs within a narrow temperature range and is complete at 400 K. Study of the profile of the curve reveals a certain asymmetry, with an ascending branch of less pronounced slope than the descending one, as corresponds to a first-order desorption process.[36,50]

The thermograms shown in Figure 4 reflect the desorption of the same dye but this time from activated charcoal with different initial coverages. These thermograms are completely different from the former ones. A

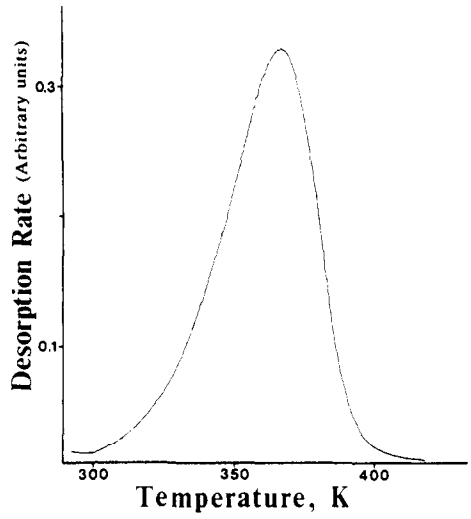

Figure 3. Desorption of crystal violet from silica gel, followed spectrophotometrically at 590 nm: ϵ_{590} = 88 800 L mol^{-1} cm^{-1}; heating rate = 2.18 K/min; flow rate = 4.5 cm^3 min; adsorbent mass = 0.0240 g; initial coverage = 3.47 × 10^{-5} mol/g.

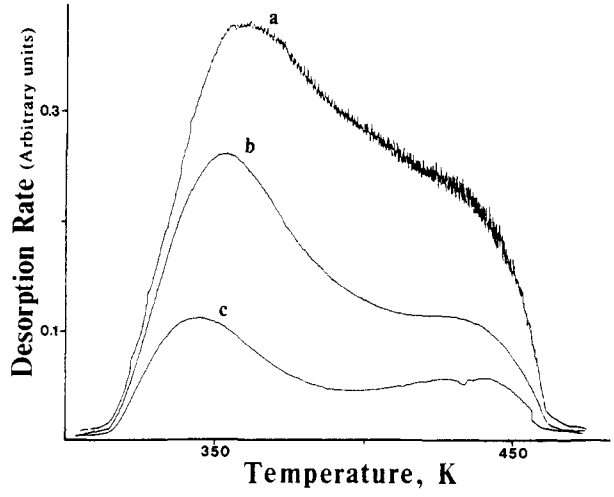

Figure 4. Desorption of crystal violet from activated charcoal as function of initial coverage, followed spectrophotometrically at 590 nm: ϵ_{590} = 88 800 L mol1^{-1} cm^{-1}; heating rate = 2.17 K/min; flow rate = 3.5 cm^3/min; (a) initial coverage = 1.81 × 10^{-4} mol/g, adsorbent mass = 0.057 g; (b) initial coverage = 9.29 × 10^{-5} mol/g, adsorbent mass = 0.086 g; (c) initial coverage = 3.75 × 10^{-5} mol/g, adsorbent mass = 0.086 g.

first maximum is observed at around 340 K, which is then displaced toward higher temperatures as the initial coverage of the samples increases. Additionally, in all of these thermograms, this first maximum is followed by a lower shoulder that extends up to 460 K; this corresponds to one or several types of adsorbent–adsorbate binding. The displacement of the first maximum as a function of the initial coverage can be attributed to several facts, essentially the occurrence of phenomena of readsorption or the existence of interactions among the adsorbed molecules, which means that the activation energy must be a function of coverage. The pronounced differences between both thermograms, Figures 3 and 4, can be accounted for in terms of a greater variety of active sites in the charcoal as compared with the silica gel.

Another example of desorption thermograms in solution is shown in Figure 5. This corresponds to the desorption from activated charcoal of phenol and some of its derivatives, *p*-nitrophenol and 2,6-dichloro-4-nitrophenol. All three compounds show a single peak, although the 2,6-

(50) Smutek, M.; Cerny, S.; Buzek, F. *Adv. Catal.* 1975, *24*, 343.

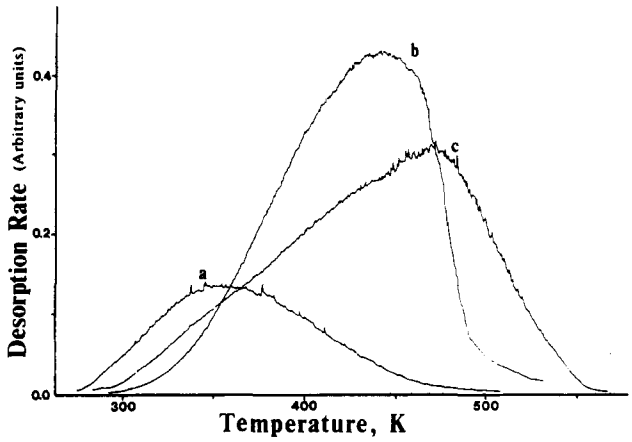

Figure 5. Desorption of phenol derivatives from activated charcoal followed spectrophotometrically: heating rate = 2.17 K/min; flow rate = 3.5 cm^3/min; (a) phenol, λ_{max} = 270 nm, ϵ_{270} = 1430 L mol^{-1} cm^{-1}, initial coverage = 5.11×10^{-3} mol/g, adsorbent mass = 0.040 g; (b) *p*-nitrophenol, λ_{max} = 319 nm, ϵ_{319} = 6700 L mol^{-1} cm^{-1}, initial coverage = 1.39×10^{-3} mol/g, adsorbent mass = 0.040 g; (c) 2,6-dichloro-4-nitrophenol, λ_{max} = 400 nm, ϵ_{400} = 10 800 L mol^{-1} cm^{-1}, initial coverage = 3.12×10^{-4} mol/g, adsorbent mass = 0.040 g.

dichloro-4-nitrophenol seems to show a shoulder at around 430 K. The corresponding maxima are displaced toward higher temperatures as the number of substituents in the phenol derivative increases, pointing to the greater binding strength by the molecules of 2,6-dichloro-4-nitrophenol. This would be consistent with the hypothesis that the –OH group would be responsible for the adsorption through a hydrogen-bonding interaction.[51] The electronegative character of the substituents would strengthen this bond, such that it would be the strongest in the case of the most substituted derivative. A study of the shape of thermograms b and c seems to point to a first-order desorption process. In the case of phenol (thermogram a), performed with a greater degree of initial coverage, once the maximum has been surpassed the thermogram becomes broader, which suggests either interactions among the adsorbed molecules or the presence of readsorption phenomena.

Discussion

From the results obtained it can clearly be seen that the TPD technique can also be extended to processes occurring in solution, with a development and parallel applications to what TPD currently has in the gaseous phase but with its own peculiar characteristics, as would correspond to the condensed state. As is known in solution, interactions between the adsorbent and the adsorbate are generally weaker than those occurring in the gas phase, where it is often possible to find numerous examples in which bonding takes place through a very strong chemical bond. This means that the temperatures required to produce desorption are relatively lower compared to those employed in gaseous phase thermograms. Additionally, desorption may also be favored by interactions between the solvent and the adsorbate. These facts are highly advantageous since in the gaseous phase there are normally no limitations to reaching high temperatures, but in the condensed phase the critical temperature of the solvent will never be surpassed. In the case of water, this temperature is relatively high (647 K), although for other solvents it is much lower.

Another fairly common characteristic in TPD in solution, as noted in the thermograms of the present work, is the great sensitivity of desorption to temperature. Small variations in temperature imply a large variation in the desorption rate. This means that the thermogram should be obtained with a very small heating rate (0.4–4.0 K/min) when compared with experiments carried out in the gaseous phase, where the heating rate may range between 10 and 1200 K/s for flash desorption. This great sensitivity makes it necessary to maintain a strict control on temperature and to have available an experimental setup able to attain very precise programming. Additionally, the use of very low heating rates implies the possibility of a better resolution of the thermogram; however, it also involves lengthy experiments that may last as long as 12 or 15 h.

Regarding the apparatus described in the present work, we believe that these requisites are fulfilled and that the results obtained are highly satisfactory. Its construction is very simple and its modular design permits the exchange of some of its parts for some other that best suits each study. Thus, the detector can be replaced by another that measures conductivity, fluorescence, refractometry, mass spectrometry, etc. Data collection is easily coupled to a computer for storage and later treatment (determination of areas, comparison of thermograms, etc.). Regarding the silicone oil bath, this can be substituted by an oven, specially when temperatures above 300 °C are required. However, the use of an oven usually involves problems in programming due to the occurrence of temperature gradients.

Until now, TPD applied to processes in the gaseous phase has proved to be a very valuable method in the elucidation of adsorption phenomena and phenomena of catalysis, yielding information about the following: (a) kinetic parameters (reaction orders, rate constants, activation parameters, etc.); (b) the chemical nature of the active sites (characterization of areas); (c) mechanisms of reaction and catalysis; (d) the nature of the adsorbent–adsorbate interaction. All these applications are also possible in processes in the condensed phase and also allow one to carry out comparative studies on adsorption and catalysis in both phases.

Registry No. Crystal violet, 548-62-9; phenol, 108-95-2; *p*-nitrophenol, 100-02-7; 2,6-dichloro-4-nitrophenol, 618-80-4.

(51) Davis, A. P.; Huang, C. P. *Langmuir* **1990**, *6*, 857.